

Synthesis of g-C₃N₄/CuO Nanocomposite as a Supercapacitor with Improved Electrochemical Performance for Energy Storage applications

Syed Khasim^{1,2,*}, Apsar Pasha³, Mohana Lakshmi⁴, Chellasamy Panneerselvam⁵, Mohammad Fahad Ullah⁶, A.A.A. Darwish^{1,2,7}, Taymour A Hamdalla^{1,2,8}, S. Alfidhli^{1,2}, S.A Al-Ghamdi^{1,2}

¹ Department of Physics, Faculty of Science, University of Tabuk, Tabuk 71491, Saudi Arabia.

² Nanotechnology Research Unit, Faculty of Science, University of Tabuk, Tabuk 71491, Saudi Arabia

³ Department of Physics, Ghousia College of Engineering, Ramanagaram, Karnataka 562 159, India.

⁴ Department of Physics, PES-University, Bangalore, Karnataka 562 159, India.

⁵ Department of Biology, Faculty of Science, University of Tabuk, Tabuk 71491, Saudi Arabia.

⁶ Department of Medical Laboratory Technology, Faculty of Applied Medical Science, University of Tabuk, Saudi Arabia

⁷ Department of Physics, Faculty of Education at Al-Mahweet, Sana's University, Al-Mahweet, Yemen

⁸ Department of Physics, Faculty of Science, Alexandria University, Egypt

*E-mail: syed.pes@gmail.com

Received: 11 May 2022 / Accepted: 12 June 2022 / Published: 4 July 2022

The quest for ever-increasing indispensable energy demands of the human race led to the design and development of novel nanomaterials for affordable, alternative energy storage structures and devices. Graphitic carbon nitride g-C₃N₄ (GCN) with unique physical and chemical properties have emerged as promising electrode material for electrochemical energy storage solutions due to its nitrogen-rich framework. However, the bare GCN has poor electrical conductivity and severe irreversible capacity loss. In this work, we report an efficient strategy to enhance the electrical and electrochemical performance of g-C₃N₄ nanocomposites decorated with copper oxide (CuO) nanoparticles. The structural, morphological, and electronic properties of as-synthesized GCN-CuO nanocomposites were systematically investigated. The presence of CuO NPs significantly contributed towards improved electrical conductivity and dielectric attributes of the composite system. The heterostructure electrodes of GCN-CuO nanocomposite exhibits superior electrochemical performance with a specific capacitance of 248 F/g @ a current density of 2 A/g. Further, the GCN-CuO nanocomposite electrodes exhibit excellent cycling stability with a capacitance retention and coulombic efficiency of 83% and 96% respectively after 5000 cycles. An energy density of 73 (Whkg⁻¹) could be achieved in these GCN-CuO nanocomposite electrodes at a power density 1662 (kWkg⁻¹). Due to superior electric, dielectric and electrochemical performances the modified electrodes based on GCN-CuO proposed in this research

could be potential candidates for high performance supercapacitors and can provide new perspectives for designing materials in energy storage applications.

Keywords: Graphitic carbon nitride, GCN-composites, Copper oxide nanoparticles, Supercapacitors, Electrochemical studies, Energy storage

1. INTRODUCTION

Energy consumption for electricity and heating will double by 2050, at most due to manufacturing, civilization, and population growth. Also, the consumption of fossil fuels (oil, coal, and natural gas) should be reduced as their extensive usage has negative environmental consequences. Advanced technologies that can store and transform energy from intermittent sources for continuous uses must be investigated to improve access to clean energy [1, 2]. Supercapacitors (SCs) and batteries have the largest possibility for electrochemical energy storage of any currently available devices. Various materials or electrocatalysts have been used to improve the storage performance, to improve storage performance, various materials or electrocatalysts have been utilized. Due to their distinctive architectures, characteristics, and remarkable performance, materials based on graphitic carbon nitride (g-C₃N₄) have sparked heated debate, particularly in recent years [3, 4]. Both SCs and batteries are widely utilized as energy storage and conversion devices. These devices have similar advantages in terms of long life and environmental friendliness and have been used to efficiently store and convert energy in solar cells, electric vehicles, and portable devices [5, 6, 7]. These two types of devices, however, nevertheless confront problems and constraints that will stymie their future advancement. SCs have a low energy density, while batteries have low energy density and modified performance. As a result, additional research on suitable electrode materials and efficient catalysts for batteries or SCs is necessary, and materials based on g-C₃N₄ are a substantial and novel candidate.

In the recent past, graphitic carbon nitride (g-C₃N₄) (GCN) as a 2D semiconducting material has gained considerable attention of researchers across the world due to its excellent physical and chemical properties such as tuneable band gap (2.7-2.8 eV), superior chemical and thermal stabilities, low-cost synthesis, natural abundance, non-toxic, improved opto-electronic characteristic properties [8, 9]. Graphitic carbon nitride (g-C₃N₄) belongs to family of 2D conjugated polymers with carbon and nitrogen in the polymer backbone. It can be synthesized from various naturally occurring carbon materials by replacing carbon atoms with that of nitrogen [10]. The graphitic carbon nitride (g-C₃N₄) also known to have lamellar structure with electrochemical features, that could be potentially used in energy storage applications. The sp² hybridized N atoms of g-C₃N₄, that has lone pair of electrons contributes to improved electrochemical performance [11]. Graphitic carbon nitride as a 2D-nanomaterial has been extensively used in many of the modern technological applications such as energy storage, optoelectronics, sensing, catalysis, and imaging [12-18]. In spite of its fascinating applications, bare-GCN has limitations such as small surface area, low conductivity, and poor chemical inertness, which hinders its suitability suitable for some of the advanced technological applications [19]. Hence, to

overcome these limitations, its structural modifications using functionalization, or to prepare nanocomposites of GCN through nano fillers has emerged as an efficient strategy [20].

Many researchers have proposed various ways to improve performance and modify the properties of g-C₃N₄, such as doping and heterogeneous interaction with other substances. Metal oxides, metal sulfides, noble metals, and carbon nanomaterials are examples of these materials [21-23]. Metal oxides are most commonly used to improve the efficiency of g-C₃N₄, for example, by increasing light absorption and decreasing electron and hole recombination by enhancing charge carrier separation. This is primarily due to the appropriate band structures [24, 25]. Recent research has shown that coordination with the carbon nitride framework by doping Fe (II) or Fe (III) improves the g-C₃N₄ catalytic performance in Fenton-like reactions over a wide pH range [17, 18, 19, 20]. A previous study committed to incorporating the transition metal cobalt into the carbon nitride framework to accelerate the iron (II) regeneration process, which effectively improves the reaction via Fe-Co on the surface of graphite carbon nitride, thus promoting the oxidation of organic compounds [21]. However, due to the potential for carcinogenicity in humans, the use of cobalt in practical applications has been limited [22]. On the other hand, the addition of Cu can effectively promote the degradation of organic materials in both homogeneous and heterogeneous systems. Copper is critical in the reduction of Fe (III) to Fe (II) in these studies [23]. Copper may also broaden the working pH range, especially in neutral or alkaline conditions, and enhance the production of reactive oxygen species (ROS) [24, 25]. Moreover, the Cu atom can be incorporated into the g-C₃N₄ matrix through interactions with the NH₂ group, resulting in the formation of stable Cu-N bonds [26].

In this context, few studies focus on developing the electrochemical properties of g-C₃N₄. The bare g-C₃N₄ has poor electrical conductivity and severe irreversible loss of capacitance. In this work, we report an effective strategy to improve the electrical and electrochemical performance of g-C₃N₄ nanocomposites decorated with Cu-Fe metallic nanoparticles. The structural, morphological, and electronic properties of the synthesized g-C₃N₄ nanocomposites were systematically investigated.

2. EXPERIMENTAL

2.1. Synthesis of graphitic carbon nitride (GCN)

Thermal decomposition technique was used to synthesize graphitic carbon nitride as reported in earlier literature with some modifications [27]. In a typical procedure, 2 gm of melamine was dissolved in 5 mL of distilled water and kept overnight at a temperature 80°C. The resulting powder was then transferred to muffle furnace and heated to 550°C for 2 hr, by ramping time of 5°C/min. The yellow-coloured final product of graphitic carbon nitride (GCN) was subjected to nano milling, finely grounded and used for further experiments.

2.2. Synthesis of GCN-CuO nanocomposite

The GCN-CuO composite was prepared by hydrothermal synthesis. In a typical procedure, 5 gm of GCN powder was dissolved in 25 mL of distilled water, the resulting suspension was sonicated for

30 min. For the synthesis of GCN-CuO nanocomposite, 1 gm of CuCl_2 and 100 mg of urea was added to the GCN solution through continuous vigorous stirring followed by sonication for 60 min. During the synthesis the pH of the above solution was modified to 10 using liquid ammonia (NH_3) and stirred for 30 min. The end solution was further transferred to a stainless-steel autoclave and kept at a temperature of 180°C for 12 hr. Finally, the resulting reaction mixture was cooled to room temperature and obtained precipitate was washed with ethanol and distilled water for several times and dried at 80°C in the vacuum oven.

2.3. Materials Characterization

The crystallographic planar structure of GCN and GCN-CuO was analyzed by using X-ray diffractometer (Ultima IV, Rigaku, Japan) with Cu $K\alpha$ radiation ($\lambda=1.540598 \text{ \AA}$). The surface functionalities of the sample were determined by Fourier Transform Infrared spectrometer (Bruker Tensor 27) within the wavenumber region of $4000\text{--}500 \text{ cm}^{-1}$. High-resolution transmission electron microscopy (JEOL JEM, 2100) operating at 200 kV was used to record the morphology of the prepared samples. The elemental composition of the sample was identified using Energy Dispersive X-ray spectroscopy (K-alpha Surface Analysis, Thermo Scientific) operating at room temperature with Al $K\alpha$ radiation as an X-ray source.

2.4. Electrical and Electrochemical measurements

For electrical measurements (conductivity and dielectric studies), the samples (GCN, GCN-CuO) were dispersed in NMP solution and spin coated onto ITO substrates as thin films. The room temperature electrical conductivity measurements were performed through four probe techniques using Keithley I-V source meter and Keithley 6487 pico ammeter/voltmeter. The room temperature dielectric measurements of the samples were carried out by two probe method using LCR impedance analyzer (Wayne Kerr-6500B London) at 100 KHz frequency. Working electrodes of GCN, GCN-CuO were prepared in terms of carbon paste electrodes. In a typical procedure, the active material, carbon paste and the binder (PVDF) were mixed in the ratio 85:15:5% in NMP solution, the resulting was slurry was drop casted on nickel foam ($1 \times 1 \text{ cm}^2$) with a mass loading of 2mg. The foam was dried in an oven at 50°C overnight before using for electrochemical tests. The cyclic voltametric (CV) tests were performed on an electrochemical workstation (CHI608E potentiostat) using a three-electrode system, comprising of carbon paste (working electrode), platinum wire (counter electrode) and Ag/AgCl (reference) in 6 M KOH at 10, 20, 30, 40 and 50 mV/s scan rate, with a potential variation of -0.8 to 0.8 V (vs Ag/AgCl electrode). The EIS studies were carried out in the frequency range of 1 Hz to 1 MHz at an AC amplitude of 5 mV.

3. RESULTS AND DISCUSSIONS

3.1. Scanning Electron Microscopy (SEM)

The morphological features of pure GCN and GCN-CuO composites studied through SEM microscopy are depicted in figure- 1 (a) and (b) respectively. The morphology of the bare GCN shows irregular granular structures at the surface with high agglomerations and formation micro-pores, the grains in GCN are not well resolved that can lead to blockage of charge carrier mobility and results in lower conductivity and poor electrochemical performance. The surface morphology of GCN-CuO nanocomposite shows partial aggregation of nanoparticles (NPs) with relatively improved homogeneous distribution of nanoparticles in the GCN matrix. The fractional surface of CuO NPs is covered with GCN which can be clearly seen from the texture of the composite samples thereby confirming the formation of heterostructure.

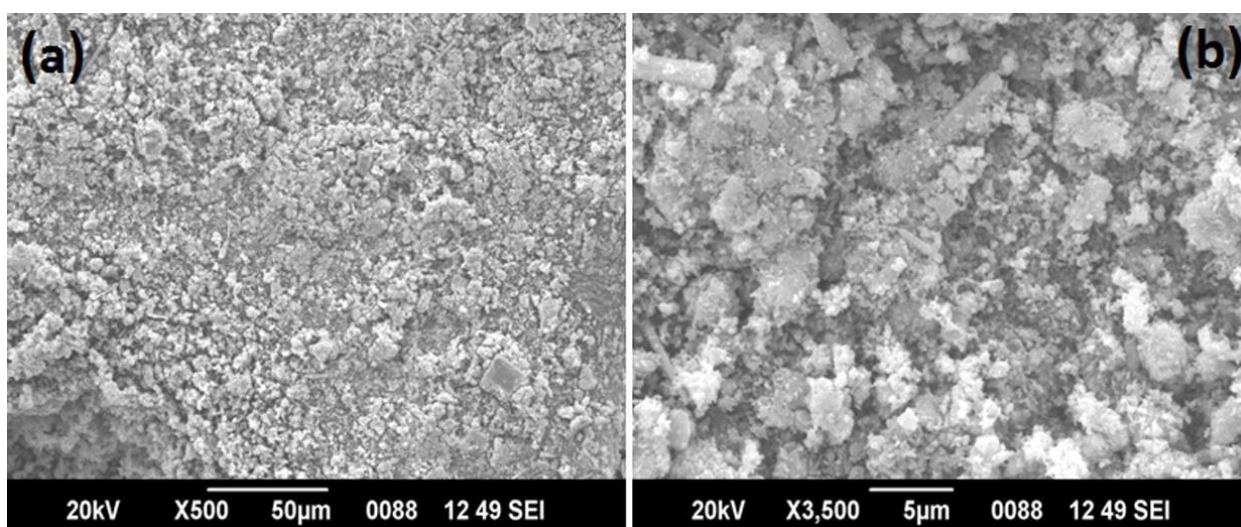


Figure 1. Scanning electron microscopic images of (a) pure GCN (b) GCN-CuO composite

3.2. Fourier transform infrared spectroscopy (FTIR)

The FTIR spectra of pure GCN and GCN-CuO composites are shown in figure-2. The two sharp signals in the pure GCN spectra at 802 and 840 cm^{-1} are in accord with the characteristic breathing pattern of the s-triazine ring system originating from polymerized C–N heterocycles [28]. The bands observed at 1210 and 2250 cm^{-1} are related to the C=N and C–N stretching vibrations respectively [29] and the broad peak at 3130 cm^{-1} is assigned to the N-H stretching vibration [30]. In the spectra of GCN-CuO, although the characteristic bands of GCN are maintained, CuO peaks are not significantly detected in composite sample which might be due to the band overlapping or vacancies between the GCN clusters. However, the variation in the intensity and a slight variation in the position of the peaks signifies a chemical bonding in the heterostructure between GCN and CuO and such structures are very much useful

for electro-electrical performance because of the easy charge carrier transfer enabled by the interconnection.

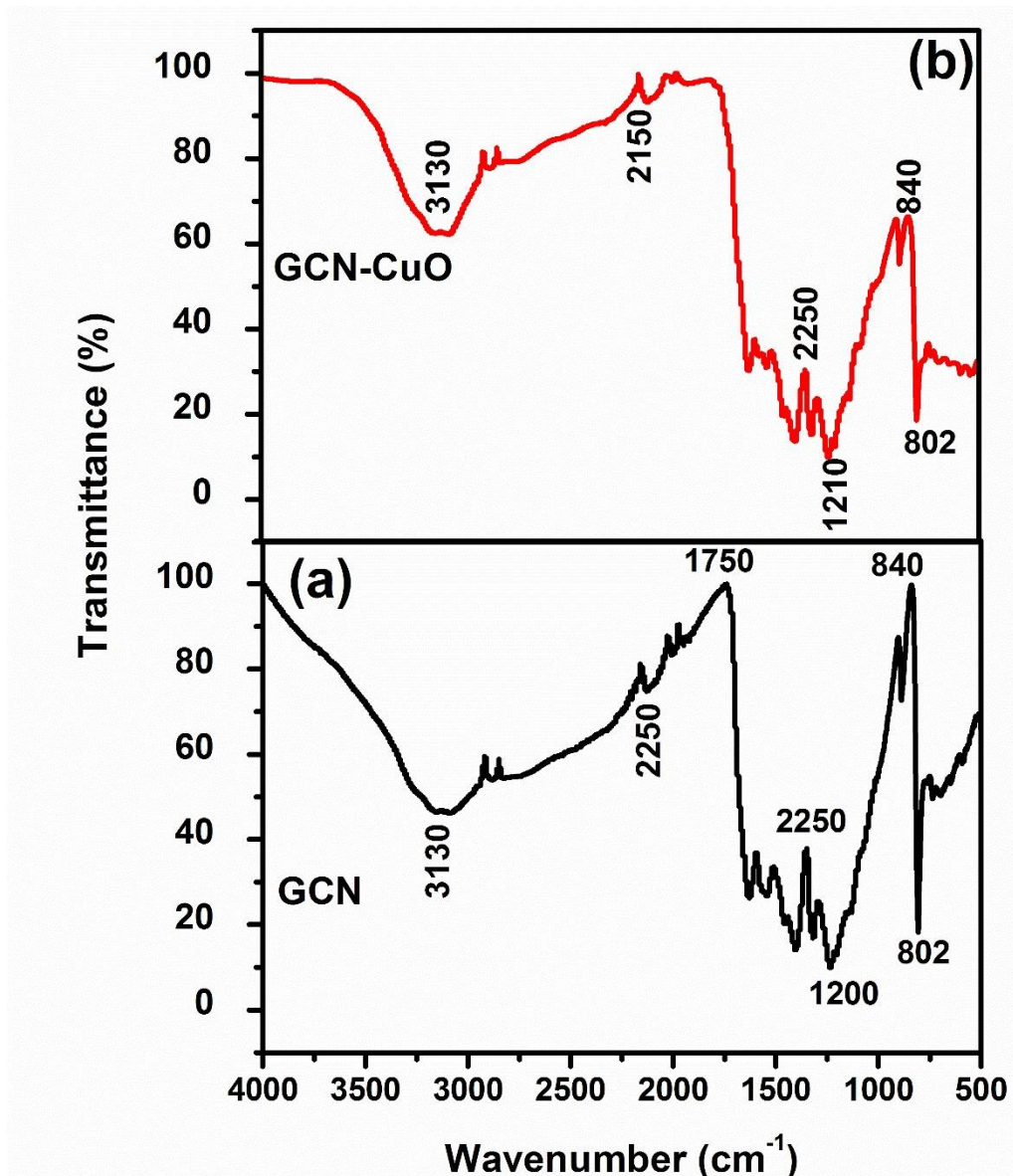


Figure 2. Fourier transforms infrared (FT-IR) spectra of pure GCN and GCN-CuO composite.

3.3. X-ray diffraction studies (XRD)

The structure and crystal phase of GCN and GCN-CuO were investigated by XRD analysis. The XRD pattern of the samples is shown in figure-3. The pattern for pure GCN showed three characteristic peaks exhibiting semi-crystalline nature. One of the peaks is strong at 27° , is indexed to the (002) diffraction plane (JCPDS Card No.: 87-1526) and is attributed to the inter-planar stacking of the conjugated aromatic systems [31]. The second one is a weak peak at 13° indexed to (100) plane and is attributed to the interlayer structural packing of the tri-s-triazine. The XRD spectra of GCN-CuO shows the presence of sharp crystalline peaks exhibiting the crystallinity of the prepared composite sample. The composite sample pattern contains many planes (110), (002), (200), (210), (211) and (300) at

diffraction peaks corresponds to $2\theta = 21^\circ, 27^\circ, 38^\circ, 44^\circ, 55^\circ$ and 62° respectively indicating successful formation of GCN-CuO heterostructure composite.

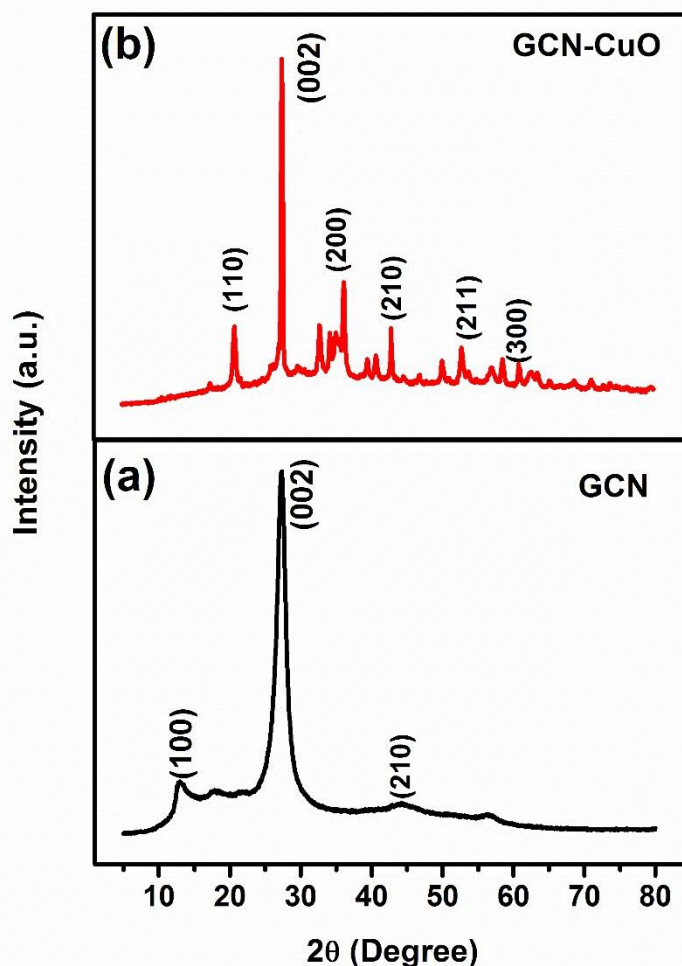


Figure 3. X-ray diffraction (XRD) spectra of pure GCN and GCN-CuO composite.

3.5. Electrical Studies

The room temperature electrical conductivity of GCN and GCN-CuO composite sample measured using four probe technique is reported in table-1. It can be inferred that the electrical conductivity of the heterostructure has increased more than ten times compared to that of pure GCN. The main reason for the enhancement in the conductivity of the composite sample may be due to a strong synergistic interaction between the organic GCN phase, which is highly electron rich and the inorganic CuO phase which has high positive ions in the lattice. This kind of combination of heterostructure is highly beneficial as it renders easy transportation of charge carriers. Combining organic and inorganic phases to form a heterostructure composite with good dielectric properties is an effective and novel approach for energy storage applications. Figure-4b represents the dielectric constant and dielectric loss of GCN and GCN-CuO samples at room temperature. From the data reported in table-1, it can be observed that the dielectric permittivity of the heterostructure GCN-CuO sample was more than double

compared to pure GCN. The improvement in the dielectric constant value arises due to increase in the polarization strength by the interfacial polarization between the two phases. Thus, incorporating CuO with high dielectric constant into the GCN matrix facilitates for high energy storage density. With the inclusion of CuO into the GCN structure, the dielectric loss drops (as shown in table-1), which benefits in the improvement of energy storage properties.

Table 1. Electrical properties of GCN and GCN-CuO nanocomposites

| Sample | Electrical Conductivity (S/cm) | Dielectric Constant | Dielectric Loss |
|-----------------------|--------------------------------|---------------------|-----------------|
| GCN | 24.5 | 28 | 1.07 |
| GCN-CuO nanocomposite | 268.2 | 64.5 | 0.45 |

3.6. Electrochemical Studies

The electrochemical properties of GCN and GCN-CuO nanocomposites were performed through CV, GCD and EIS techniques using three electrode system. The CV curves were recorded for both GCN and GCN-CuO nanocomposites with different scan rates ranging from 10 mV/s to 50 mV/s as shown in figure-4 (a, b). Visible and well distinguished redox peaks in GCN-CuO nanocomposites shows excellent pseudo capacitance behaviour of the composite in comparison to bare GCN. Transformation of CV curve shapes into quasi-rectangular in case of GCN-CuO nanocomposites further confirms the fact that, the charge storage mechanism in these composites is due to ELDC and Faradaic reaction (Cu/Cu^{2+}) in the potential range -0.8V to +0.8V. It also interesting to note that the shapes of CV curves of the composite don't change with scan rates, indicating excellent electrochemical stability and reversibility of the electrodes. The CV curves of GCN-CuO composites shows increased current response and larger area with scan rates indicating capacitance. The superior electrochemical performance of the composites with different scan rates are mainly due to the combination of improved surface area or defect sites and ion exchange among the heterostructures [32]. The composite formation in heterostructures of GCN-CuO facilitates improved electronic charge transfer pathways that causes more diffusion of K^+ ions.

The charge transfer resistance of GCN and GCN-CuO sample using Electron Impedance Spectroscopy (EIS) is presented in figure-5a. The semi-circular arc radius in the Nyquist plots signifies the transportation and electron transfer resistance of the interface layer. The smaller the arc radius, the lower the charge transfer resistance and vice-versa. It can be observed from the plot, that the arc radius for the GCN-CuO sample is smaller than pure GCN implying improvement in the transportation of charge carriers at the interface.

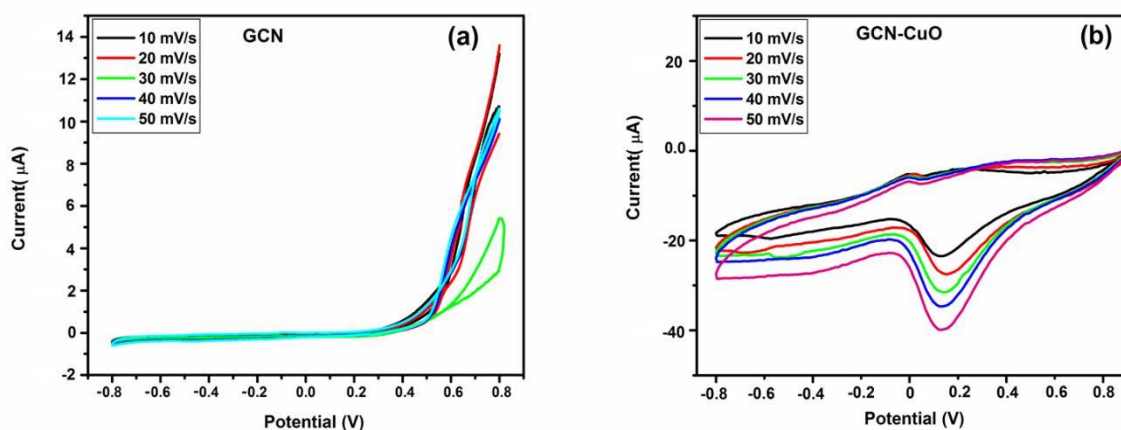


Figure 4. Cyclic Voltammetry (C-V) curves at different scan rates for (a) GCN and (b) GCN-CuO composite in 6 M KOH for scan rates 10 to 50 mV/s, with a potential variation of -0.8 to 0.8 V (vs Ag/AgCl electrode).

The GCN-CuO heterostructure exhibited an excellent response to charge transfer with reduced electrical resistivity and is attributed to the intimate interfacial interaction between GCN and CuO phases which is conducive for enhancing the electrical properties of the optimized sample. The variation of current density as function of applied potential for GCN and GCN-CuO nanocomposites is depicted in figure-5b. It is interesting to note that the GCN-CuO nanocomposites shows significant enhancement in the current density with applied potential indicates the transformation of composite into more conducting nature in comparison to bare GCN. Higher current density in the composite is attributed due to the improved catalytical activity of nanocomposite. The presence of CuO NPs in GCN facilitates improved active sites for the charge transportation which results into enhanced current density and conductivity. These results further support for increased conductivity as observed in case of DC conductivity and EIS results (table-1 & figure-5a). Mott-Schottky plots of GCN and GCN-CuO nanocomposites were evaluated based on EIS data to investigate the flat band potentials and the electronic nature of the samples using the equations mentioned in the previous work [33]. Both GCN and GCN-CuO nanocomposites shows linear behaviour for Mott-Schottky plots (as shown in figure-5c) indicates perfect semiconducting nature of the samples. The positive slope of the Mott-Schottky plots in both GCN and GCN-CuO nanocomposites indicates n-type semiconducting behaviour of the composites. The extrapolation of Mott-Schottky plots on x-axis indicates the flat band potential, from the plots it is observed that the GCN-CuO nanocomposite shows reduced flat band potential in comparison to bare GCN which suggests reduced band gap in the GCN-CuO nanocomposites. The Mott-Schottky plots further confirms the reduced band gap and increased conductivity in case of GCN-CuO nanocomposites which strongly confirms the previous data on electronic properties (conductivity, EIS and results) of the composites.

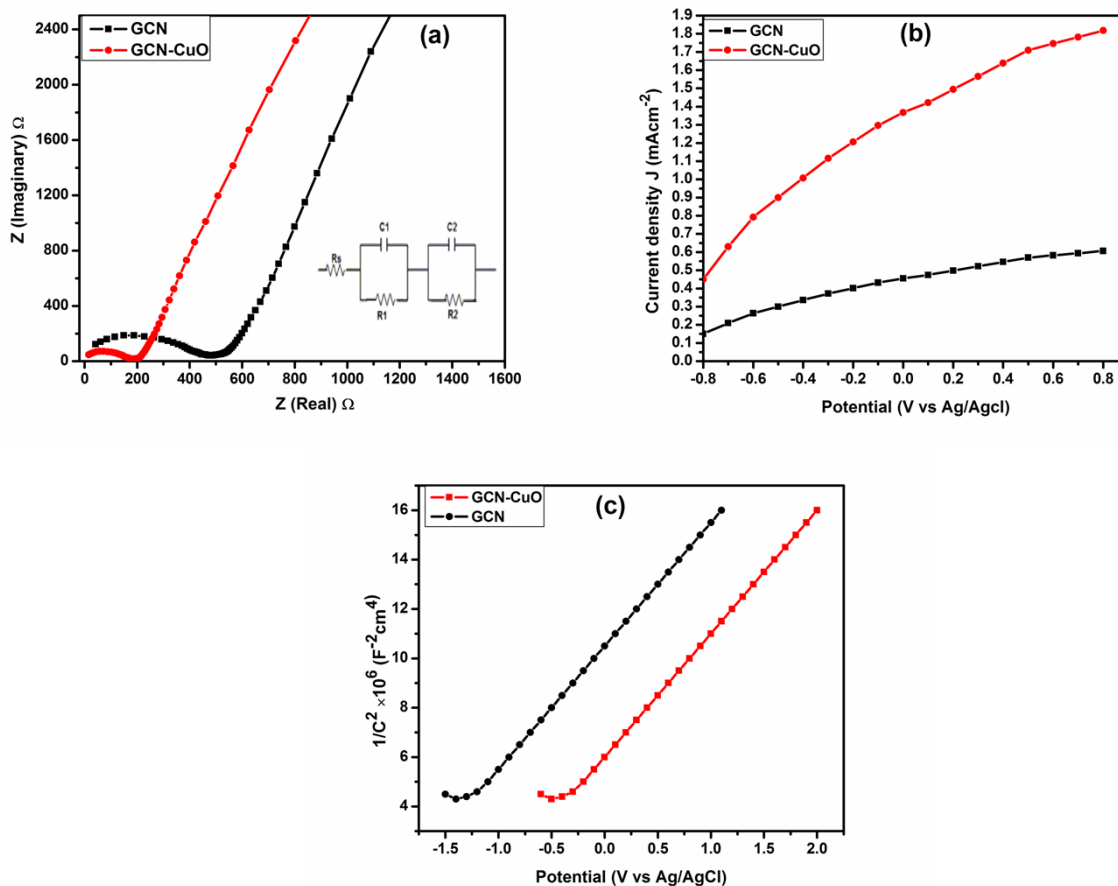


Figure 5. (a) Nyquist Plots from Electrochemical Impedance Spectroscopy (EIS) for GCN and GCN-CuO composites (b) current density as a function of electrochemical potential for GCN and GCN-CuO composites (c) Mott-Schottky plots for GCN and GCN-CuO composites

The specific capacitance (C_{sp}) of GCN and GCN-CuO nanocomposite electrodes were investigated using GCD technique at a current density of 1 A/g and is represented in figure-6a. Slightly nonlinear and asymmetric response of charge-discharge curve confirms the pseudocapacitive behavior of the samples. The GCN-CuO nanocomposite shows longer discharge time in comparison to bare GCN which suggests a very small solid/liquid interface resistance, minimum energy loss and higher C_{sp} values for the composite electrode. It is interesting to note that the C_{sp} values for GCN-CuO nanocomposite is 2.1 times greater than that of bare GCN at a current density of 2 A/g (248 F/g for GCN-CuO v/s 112 F/g for bare GCN) as shown in figure-6b, which further supports for enhanced C_{sp} values as observed through GCD curves. The improved specific capacitance of GCN-CuO nanocomposite may be attributed due to (i) improved synergistic effects between CuO nanoparticles and thin sheets of GCN (ii) the migration of ions at the interfaces between CuO NPs and GCN (iii) enhanced specific area of the nanocomposite (iv) availability of large number of active sites due the presence of CuO NPs and (v) presence of CuO NPs facilitates the reaction rate and reaction kinetics. The decrease in specific capacitance of figure-6b with current density is mainly due to the inadequate migration of K⁺ ions in the

in the electrode interface and limited time to access the active sites in the nanocomposite electrode. The electrochemical diffusion phenomena can further be well understood with the specific capacitance of GCN and GCN-CuO electrodes at different scan rates represented in figure-6c. The specific values decreased at higher scan rates due to increased current density resulting from the diffusion effect of the ions [34]. The electrode surface consists of active and inactive sites. At lower scan rates there will be increased participation of active sites in electrochemical reaction, resulting into higher capacitance. Whereas at higher scan rates the electrolyte ions may not have enough time to diffuse into electrode material resulting into lower accumulation of charges and decrease in specific capacitance [35]. At low scan rates the samples show improved specific capacitance than at the higher scan rates. The GCN-CuO nanocomposite electrode offers higher specific capacitance than bare GCN for the all the scan rates, which further supports the observations of CV curves. The improved specific capacitance at low scan rates is due to higher diffusion of ions in the electrodes, at higher scan rates the ions fail to diffuse within the electrode in a given time and hence the C_{sp} values decreases.

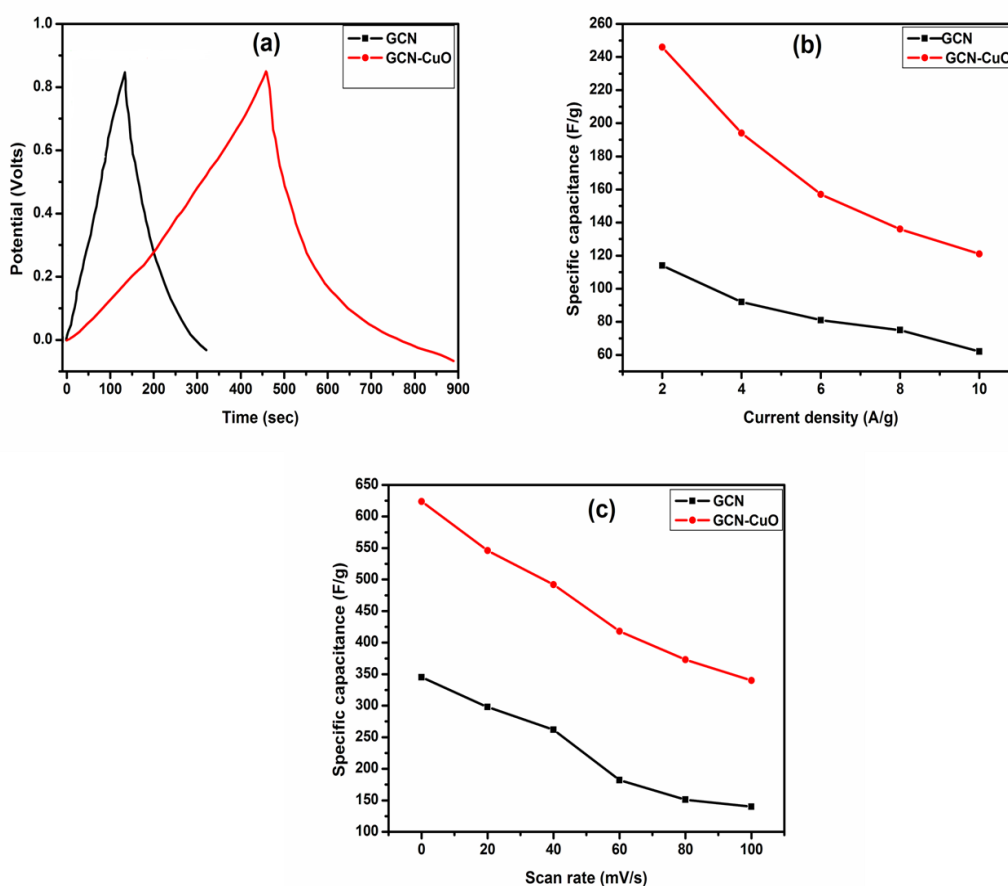


Figure 6. (a) Galvanostatic Charge-Discharge (GCD) curves for GCN and GCN-CuO composites (b) variation of specific capacitance with current density for GCN and GCN-CuO composites (c) variation of specific capacitance with scan rate for GCN and GCN-CuO composites

The variation of energy density as a function power density for GCN and GCN-CuO nanocomposites was investigated and represented in terms of Ragone plots as shown in figure-7a. The GCN-CuO nanocomposite has achieved a maximum energy density of 73 (Whkg^{-1}) v/s 44 (Whkg^{-1}) for bare GCN at a power density 1662 (kWkg^{-1}). Stability, capacitance retention, durability and cycling ability are key parameters to analyse the performance of electrochemical supercapacitors. The stability of the electrode materials in terms of their cycling capacity was investigated for both GCN and GCN-CuO nanocomposites as depicted in figure-7b. The GCN-CuO nanocomposite electrode shows excellent cycling ability with a capacity retention of 83% after 5000 cycles in comparison to 41% for the bare GCN. This indicates that the bare GCN undergoes high volume change during when exposed to different cycles of charging and discharging. In addition, the GCN-CuO nanocomposite electrode exhibits a coulombic efficiency of 96% after 5000 cycling performances in comparison to 63% for bare GCN as indicated in figure-7c. The GCN-CuO modified electrode used in this investigation exhibits superior electrochemical performance for the fabrication of supercapacitors in comparison to recent literature on GCN-based composites as summarized in table-2.

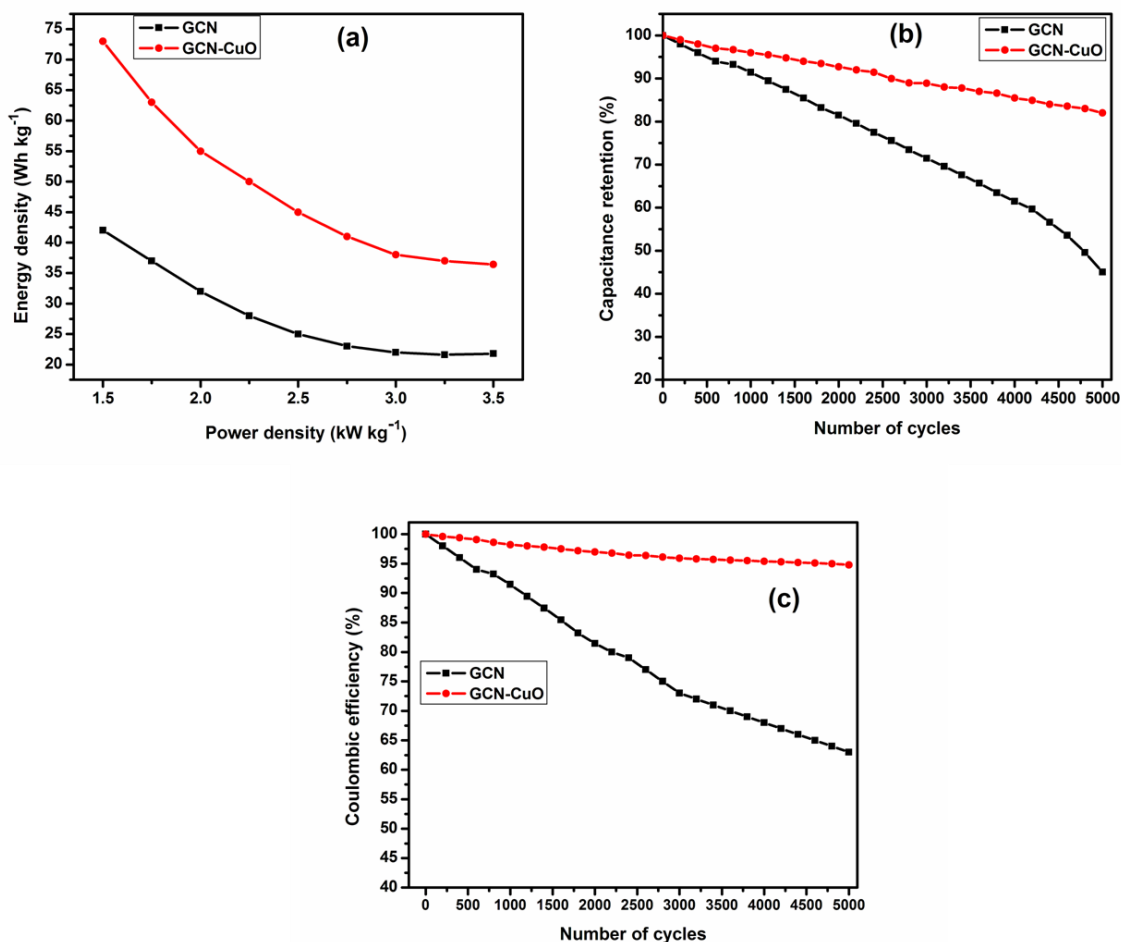


Figure 7. (a) Ragone plots for GCN and GCN-CuO composites (b) Capacitance retention for GCN and GCN-CuO composites (c) Coulombic efficiency for GCN and GCN-CuO composites

Table 2. Performance of Graphitic carbon nitride-based supercapacitors in recent literature

| Electrochemical Platform | Methods used | Conductivity (S/cm), DEC | Capacitance (Fg ⁻¹), CD (Ag ⁻¹) | CR, CN | Reference |
|---|-----------------------------|--------------------------|---|-------------|--------------|
| MnO ₂ /g-C ₃ N ₄ NC | Soft chemical route | ---- | 211, 1 | ---- | 36 |
| TiO ₂ /g-C ₃ N ₄ | Hydrothermal | ---- | 125.1, 1 | 100%, 1000 | 37 |
| Fe ₂ O ₃ /g-C ₃ N ₄ | Solvothermal | ---- | 260, 0.5 | ---- | 38 |
| MoS ₂ /g-C ₃ N ₄ | Mechanical Milling | ---- | 240.85, 1 | ---- | 39 |
| PEDOT-PSS/g-C ₃ N ₄ | Layer-by-Layer Assembly | ---- | 200, 2 | 96.6%, 1000 | 40 |
| GCN-NF | Polymerization | ---- | 263.75, 1 | 93.2%, 2000 | 41 |
| Tubular GCN | Pre-treatment of melamine | ---- | 233, 0.2 | 90%, 1000 | 42 |
| GCN | Melamine | ---- | 71, 0.5 | ---- | 41 |
| g-C ₃ N ₄ /CuMnO ₂ | Single step reduction | ---- | 200, 1 | 91%, 1000 | 43 |
| C doped g-C ₃ N ₄ /MnO ₂ | Hydrothermal | ---- | 324, 0.2 | 80.2%, 1000 | 44 |
| g-C ₃ N ₄ /ZnCO ₂ O ₄ | Hydrothermal | ---- | 150, 4 | 90%, 2500 | 45 |
| g-C ₃ N ₄ /SnS ₂ | Solvothermal | ---- | 178, 1 | 82%, 1500 | 46 |
| g-C ₃ N ₄ /CuO NPs | <i>in situ</i> Hydrothermal | 273.4, 42.5 | 248, 2 | 83%, 5000 | Present Work |

DEC- Dielectric constant, CD- Current Density, CR- Capacitance Retention, CN- Cycle Number

4. CONCLUSIONS

Herein, a heterostructure electrode material based on copper oxide nanoparticles (CuO) grafted over g-C₃N₄ (GCN) sheets has been synthesized successfully and utilized in fabricating a supercapacitor for energy storage applications. Materials characterization techniques such as SEM, FTIR and XRD confirms the successful formation of GCN-CuO nanocomposite due to synergetic interaction between GCN and CuO phases. The presence of CuO NPs significantly contributed towards improved electrical conductivity and dielectric attributes of the composite system. The electrochemical impedance spectroscopy results further confirm the enhanced conductivity in GCN-CuO nanocomposites, whereas Mott-Schottky plots suggests n-type semiconducting nature of the prepared nanocomposites. The heterostructure electrodes of GCN-CuO nanocomposite exhibits superior electrochemical performance with a specific capacitance of 248 F/g @ a current density of 2 A/g. Further, the GCN-CuO nanocomposite electrodes exhibit excellent cycling stability with a capacitance retention and coulombic efficiency of 83% and 96% respectively after 5000 cycles. An energy density of 73 (Whkg⁻¹) could be achieved in these GCN-CuO nanocomposite electrodes at a power density 1662 (kWkg⁻¹). Due to superior electric, dielectric and electrochemical performances the modified electrodes based on GCN-

CuO proposed in this research could be potential candidates for high performance supercapacitors and can provide new perspectives for materials in energy storage applications.

CREDIT AUTHORSHIP CONTRIBUTION STATEMENT

Syed Khasim - Conceptualization, Methodology, Experimentation, Data analysis, Writing: Apsar Pasha & Mohana Lakshmi - Methodology, Writing final Draft: AAA Darwish, Taymour Hamdallah, S.A. Al-Ghamdi & Shahad Alfadli - Analysis of Materials Characterization and Electric properties: Chellasamy Paneerselvam & Mohammad Fahad Ullah - Electrochemical analysis. Author S. K would like to thank Prof. Kumar M and Prof. M.N Gouda for their valuable discussions and suggestions.

DECLARATION OF COMPETING INTEREST

The authors declare that they have no known competing financial interests or personal relationships that could have appeared to influence the work reported in this paper.

ACKNOWLEDGEMENTS

The authors would like to acknowledge financial support for this work, from the Deanship of Scientific research (DSR), University of Tabuk, Tabuk, Saudi Arabia, under Grant No. S-1441-0157.

References

1. L. Zhang, S. Zheng, L. Wang, H. Tang, H. Xue, G. Wang and H. Pang, *Small*, 13 (2017) 1700917.
2. K. Liao, P. Mao, N. Li, M. Han, J. Yi, P. He, Y. Sun and H. Zhou, *J. Mater. Chem., A* 4 (2016) 5406.
3. P. Wen, P. Gong, J. Sun, J. Wang and S. Yang, *J. Mater. Chem., A* 3 (2015) 13874.
4. Y. Huang, J. Huo, S. Dou, K. Hu, and S. Wang, *RSC Adv.*, 6 (2016) 66368.
5. S. Khasim, N. Badi, A. Pasha, S.A. Al-Ghamdi, N. Dhananjaya, S. Pratibha, *Int. J. Electrochem. Sci.*, 16 (2021) 210227
6. J. Ma, X. Guo, Y. Yan, H. Xue and H. Pang, *Adv. Sci.*, 5 (2018) 1700986.
7. S. Khasim, A. Pasha, N. Badi, M. Lakshmi and Y.K. Mishra, *RSC Adv.*, 10 (2020) 10526
8. W.J. Ong, L.L. Tan, Y.H. Ng, S.T. Yong, S.P. Chai, *Chem. Rev.*, 116 (2016) 7159.
9. G. Yanalak, F. Doganay, Z. Eroglu, H. Kucukkececi, E. Aslan, M. Ozmen, S.Z. Bas, O. Metin, I. Hatay Patir, *Appl. Sur. Sci.*, 557 (2021) 149755.
10. H. Dai, S. Zhang, G. Xu, L. Gong, Mei Fu, X. Li, S. Lu, C. Zeng, Y. Jiang, Y. Lin and G. Chen, *RSC Adv.*, 4 (2014) 11099.
11. J. Tian, Q. Liu, C. Ge, Z. Xing, A.M. Asiri, A.O. Al-Youbi and X. Sun, *Nanoscale*, 5 (2013) 8921.
12. W.J. Ong, L.L. Tan, S.P. Chai, S.T. Yong, A.R. Mohamed, *Nano Energy*, 13 (2015) 757.
13. B. Li, C. Lai, G. Zeng, D. Huang, L. Qin, M. Zhang, M. Cheng, X. Liu, H. Yi, C. Zhou, *Small*, 15 (2019) 1804565.
14. X. Zhang, X. Xie, H. Wang, J. Zhang, B. Pan, Y. Xie, *J. Am. Chem. Soc.*, 135 (2012) 18.
15. G.W. Woyessa, J.B. dela Cruz, M. Rameez, C.H. Hung, *Appl. Catal., B* 291 (2021) 120052.
16. M.G. Ashritha, K. Hareesh, *Journal of Energy Storage*, 32 (2020) 101840.
17. S. Bonyadi, K.H. Ghanbari, M. Ghiasi, *New J. Chem.*, 44 (2020) 3412.
18. S. Khasim, H.M. Almutairi, S.E. Albalawi, A.S. Alanazi, O.A. Alshamrani, A. Pasha, A. A. A. Darwish, T.A. Hamdalla, C. Panneerselvam, S. A. Al-Ghamdi, *J. Inorg. Organomet. Polym. Mater.*, <https://doi.org/10.1007/s10904-022-02334-9>
19. Y. Wang, X. Wang, M. Antonietti, *Angew. Chem. Int. Ed.* 51 (2012) 68.
20. L. Liu, M. Wang, C. Wang, *Electrochim. Acta*, 265 (2018) 275.

21. H. Jiang, Y. Li, D. Wang, X. Hong, B. Liang, *Curr. Org. Chem.*, 24 (2020) 673.
22. Y. Ren, D. Zeng, Ong, W.J. Chin. *J. Catal.*, 40 (2019) 289.
23. L. Wang, C. Wang, X. Hu, H. Xue, H. Pang, *Chem. Asian J.*, 11 (2016) 3305.
24. C. Liu, Y. Qiu, J. Zhang, Q. Liang, N. Mitsuzaki, Z. Chen, *J. Photochem. Photobiol., A* 371 (2019) 109.
25. W. Zou, B. Deng, X. Hu, Y. Zhou, Y. Pu, S. Yu, K. Ma, J. Sun, H. Wan, L. Dong, *Appl. Catal., B* 238 (2018) 111.
26. J. Zhu, X. Zhu, F. Cheng, P. Li, F. Wang, Y. Xiao, W. Xiong. *Appl. Catal., B* 256 (2019) 117830.
27. Z. Zhao, Y. Ma, J. Fan, Y. Xue, H. Chang, Y. Masubuchi, S. Yin, *J. Alloys. Comp.*, 735 (2018) 1297.
28. M. Bledowski, L. Wang, A. Ramakrishnan, O.V. Khavryuchenko, V.D. Khavryuchenko, P.C. Ricci, J. Strunk, T. Cremer, C. Kolbeck, R. Beranek, *Phys. Chem. Chem. Phys.*, 13 (2011) 21511.
29. M. Ovcharov, N. Shcherban, S. Filonenko, A. Mishura, M. Skoryk, V. Shvalagin, V. Granchak, *Mater. Sci. Eng., B* 202 (2015) 1.
30. R. Mohini, N. Lakshminarasimhan, *J. Mater. Res. Bull.*, 76 (2015) 370.
31. S.W. Zhang, J.X. Li, M.Y. Zeng, J.Z. Xu, X.K. Wang, W.P. Hu, *Nanoscale*, 6 (2014) 4157. 32.
32. Yuqing Luo, Yan Yan, Shasha Zheng, Huaiguo Xue and Huan Pang, *J. Mater. Chem., A* 7 (2019) 901
33. S. Wojtyła, K. Śpiewak, T. Baran, *J. Inorg. Organomet. Polym. Mater*, 30 (2020) 3418.
34. S. Yesmin, M. Devi, I. Hussain, R. Dasgupta, Siddhartha S. Dhar, *J. Energy Storage.*, 44 (2021) 103308
35. J. Yan, J. Liu, Z. Fan, T. Wei, L. Zhang, *Carbon*, 50 (2012) 2179.
36. X. Chang, X. Zhai, S. Sun, D. Gu, L. Dong, Y. Yin and Y. Zhu, *Nanotechnology*, 28 (2017) 135705.
37. Y. Zhao, L. Xu, S. Huang, J. Bao, J. Qiu, J. Lian, L. Xu, Y. Huang, Y. Xu and H. Li, *J. Alloys. Compd.*, 702 (2017) 178.
38. L. Xu, J. Xia, H. Xu, S. Yin, K. Wang, L. Huang, L. Wang and H. Li, *J. Power Sources.*, 245 (2014) 866.
39. S. A. Ansari and M. H. Cho, *Sci. Rep.*, 7 (2017) 43055.
40. X. Chen, X. Zhu, Y. Xiao and X. Yang, *J. Electroanal. Chem.*, 743 (2015), 99.
41. M. Tahir, C. Cao, N. Mahmood, F. K. Butt, A. Mahmood, F. Idrees, S. Hussain, M. Tanveer, Z. Ali and I. Aslam, *ACS Appl. Mater. Interfaces.*, 6 (2014), 1258.
42. M. Tahir, C. Cao, F. K. Butt, F. Idrees, N. Mahmood, Z. Ali, I. Aslam, M. Tanveer, M. Rizwan and T. Mahmood, *J. Mater.Chem., A* 1 (2013) 13949.
43. S.S. Siwal, Q. Zhang, C. Sun and V.K. Thakur, *Nanomaterials*, 10 (2020) 2.
44. Q.Y. Shan, B. Guan, S.J. Zhu, H.J. Zhang and Y.X. Zhang, *RSC Adv.*, 6 (2016) 83209.
45. M. Sharma and A. Gaur, *Sci.Rep.*, 10 (2020) 2035.
46. S.A. Ansari and M. H. Cho, *Sustainable Energy Fuels*, 1 (2017), 510.